Astron. Astrophys. 330, 1180–1189 (1998)

ASTRONOMY AND ASTROPHYSICS

Two-body relaxation in softened potentials

Christian Theis

Institut für Astronomie und Astrophysik der Universität, Olshausenstr. 40, D-24098 Kiel, Germany (theis@astrophysik.uni-kiel.de)

Received 30 June 1997 / Accepted 27 October 1997

Abstract. Semi-analytical calculations for the two-body relaxation in softened potentials are presented and compared with N-body simulations. With respect to a Keplerian potential the increase of the relaxation time in the modified potentials is generally less than one order of magnitude, typically between 2 and 5, if the softening length is of the order of the mean interparticle distance. A comparison between two frequently applied softening schemes, one based on a Plummer mass distribution, the other defined by a spline interpolation on a compact support, shows that the spline-based procedure gives for the same central potential depth systematically smaller increases, but the differences between both are only of the order of 20-40%. If the softening length of the spline based scheme is twice the Plummer softening length, the relaxation rates become almost identical. A simple model that assumes that the influence of softening can be described by neglecting all deflections, if the impact parameter is less than the softening length, and otherwise uses Keplerian orbits, is within a factor of 2 in agreement with the detailed calculations. Measuring the relaxation times by N-body simulations gives a fair agreement with the semi-analytical results and, also with the simple model. In order to reproduce the measured relaxation time ratios the upper limit $p_{\max}$ of the impact parameter used to calculate the Coulomb logarithm must be chosen of the order of the system's size instead of the mean interparticle distance which corroborates the results of Farouki & Salpeter (1982, 1994).

Key words: stellar dynamics – methods: numerical – globular clusters: general – galaxies: kinematics and dynamics

1. Introduction

In all stellar systems such as globular clusters or galaxies direct encounters between stars or other constituents of the N-body system lead to a change of their velocity distribution. This kind of relaxation is mainly due to the cumulative effect of small angle encounters which are measured by a relaxation time τ (Chandrasekhar, 1942). Roughly speaking, after a time τ the squared mean change of the velocity becomes equal to the mean squared velocity, i.e. the memory of the initial velocity is lost. In case of a virialized system Spitzer & Hart (1971) derived the simple relation $\tau/\tau_{\rm d} \approx 0.04N/\log(0.4N)$ between the relaxation time, the dynamical time $\tau_{\rm d}$ and the number N of particles in the system. Though many approximations such as equal mass particles or homogeneity and virialization of the N-body system are made, this relation is widely applied for first estimates of the two-body relaxation time even for systems not fitting these conditions very well. E.g. in case of King models Theuns (1996) has demonstrated a fair overall agreement between theoretical and experimental energy diffusion coefficients emphasizing, however, that in some regions deviations by a factor up to 2 are found.

The dependence of the relaxation time on N shows a strong, almost linear increase of the ratio τ / $\tau_{\rm d}$ with N starting from 2.5 for N = 100 to 111 for N = 10^4 and up to $3.8 \cdot 10^8$ for a typical number N = 10^{11} of stars in a galaxy. Thus, in an elliptical galaxy two-body relaxation is almost negligible within a Hubble time, because the typical dynamical time is of the order of 10^8 yrs. Similar arguments hold in principle also for disk galaxies. However, the fact that the velocity dispersion in the disk is much smaller than the corresponding virial values results in stronger two-body interactions and thus a decrease of the relaxation time. Whether the relaxation time of disk-like systems and the corresponding numerical models becomes as small as the rotation period has been controversally discussed by many authors (Rybicki 1971, Hohl 1973, Mishurov 1984, White 1988).

For several decades N-body simulations have been used as a theoretical tool to understand the dynamics of stellar systems. Though the most desirable simulation would use as many particles as constituents in the real N-body system, most numerical models are restricted to 10^3 up to 10^7 particles depending on the required accuracy and the applied method. Thus, the (artificial) relaxation arising in these simulations can generally be several orders of magnitude stronger than the relaxation in the real N-body system. If the simulation time is shorter than this artificial relaxation time, the system evolves like a collisionless system and the results of the simulation should be reliable with respect to relaxation effects. For example, a simulation with N = 10^4 particles should allow for the collisionless evolution of an el-

Send offprint requests to: Ch. Theis

liptical galaxy over 1 or 2 Gyr, afterwards artificial relaxation processes commence to become important. In more structured and cold dynamical systems like galactic disks or the relatively low N galactic centers however, the artificial relaxation time can become quite small and results can be affected already after a few dynamical timescales (e.g. Rybicki 1971, White 1988). For instance, after a few revolutions an initially thin, cold disk is dynamically heated and the scale height of the disk is increased (Quinn et al. 1993).

In order to avoid this artificial effect there are basically two possibilities: The more favourable one is to increase N in the simulation. Unfortunately, in direct integration schemes the computational costs vary between $N \log N$ and N^2 which prohibits generally very large N. Another possibility is to modify the law of gravity, i.e. to soften the gravitational encounter on a scale length ϵ. Thus, the deflection of the orbits of two interacting particles and also the change rate of the velocities become smaller resulting in an enhanced relaxation timescale. The basic requirements for a softening procedure are that it should first avoid the Keplerian divergence of the gravitational attraction for small distances and second it should be identical to the Keplerian force at large distances. In principle, there is an infinite number of such softening schemes, practically only a few are used. Probably the most popular and also the oldest one is the scheme introduced by Aarseth (1963) which applies the potential of a Plummer model

$$\phi_{\rm P}(r) = -\frac{Gm_{\rm f}}{\epsilon} \cdot \left(1 + (r/\epsilon)^2\right)^{-1/2} , \qquad (1)$$

where $m_{\rm f}$ is the mass of an arbitrary *field* star, r the distance to the field star and G the constant of gravity. The *softening length* ϵ gives a typical scale on which the potential strongly deviates from the Keplerian potential. The basic advantage is its simplicity as well as the simple interpretation as a mass smeared out according to a Plummer density distribution. Especially for the potential of extended objects like molecular clouds Eq. (1) might give a first approximation.

A disadvantage is that the deviation from the Keplerian potential extends to infinity though becoming vanishingly small. Spline based softening procedures like the one suggested by Hernquist & Katz (1989) can avoid this difficulty, because they only differ from the Keplerian potential on a compact support with a radius 2 $\epsilon_{\rm sp}$:

$$\phi_{\rm S}(r) = -Gm_{\rm f} \cdot f(r) \qquad (2)$$

with

$$f(r) = \begin{cases} -\frac{2}{\epsilon_{\rm sp}}\left[\frac{x^2}{3} - \frac{3x^4}{20} + \frac{x^5}{20}\right] + \frac{7}{5\epsilon_{\rm sp}} & 0 \le x < 1 \\ -\frac{1}{15r} - \frac{1}{\epsilon_{\rm sp}}\left[\frac{4x^2}{3} - x^3 + \frac{3x^4}{10} - \frac{x^5}{30}\right] + & \\ +\frac{8}{5\epsilon_{\rm sp}} & 1 \le x < 2 \\ \frac{1}{r} & x \ge 2 \end{cases} \qquad (3)$$

and $x \equiv r/\epsilon_{\rm sp}$. The potential distributions with both softening recipes are shown in Fig. 1. Other softening procedures like the homogeneous sphere kernel or even an anisotropic softening using a homogeneous ellipsoid kernel have been discussed by Pfenniger & Friedli (1993). Concerning the actual choice of the softening length there are only a few investigations for special mass distributions (e.g. Merritt 1996, Romeo 1994, 1997). Though for some particle configurations the practical applicability of the derived criteria has been demonstrated (e.g. for galactic disks by Junqueira & Combes 1996), a simple (i.e. local) criterion for a general choice of ϵ, which is suited for arbitrary N-body configurations, is not known and may not exist.

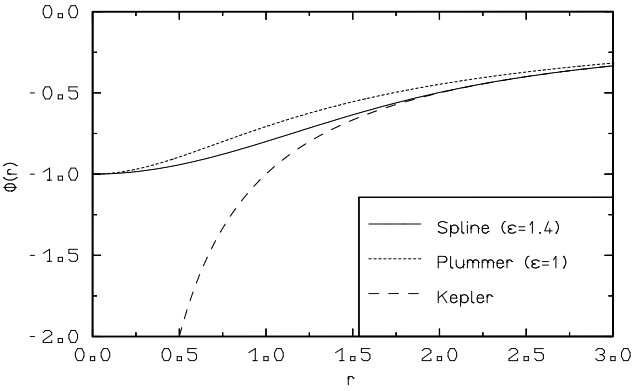

Fig. 1. Radial dependence of the softened and the Keplerian potentials. The radius is normalized to the Plummer softening length ϵ. The softening length $\epsilon_{\rm sp}$ in the spline-based models is a factor 7/5 larger than ϵ giving the same central potential depth as for the Plummer softening.

Another possibility to overcome the two-body relaxation is to use indirect N-body schemes like the particle-mesh methods (e.g. van Albada, 1986) or the expansion schemes (Clutton-Brock, 1973, Hernquist & Ostriker, 1992). These methods allow the largest number of particles in N-body simulations, however, they suffer from a lower flexibility compared to direct methods. Though the two-body relaxation in these schemes is stronger suppressed than in direct schemes, they exhibit relaxation like in more collisional schemes (Hernquist & Barnes 1990). Weinberg (1993) argued that the similar relaxation rates measured by direct and indirect N-body methods are due to collective effects. In this case the relaxation rates should not strongly depend on the details of the local softening procedure.

Since the relaxation in the indirect schemes depends much more on the implementation of the code, i.e. the number of grid cells, the density calculation scheme or the applied (truncated) set of basis functions, I restrict myself here to direct N-body codes and the two introduced softening procedures, the Plummer softening and the spline softening. Different to previous studies of relaxation I calculate the relaxation rates based on the detailed orbits in the modified potentials *directly* according to Spitzer's (1987) definition instead of measuring it by N-body simulations of special configurations. In addition to the much cheaper computational costs and the more rigorous direct treatment this has the advantages that first the results can be compared directly with the analytical results for the Keplerian force law and second they do not depend on special features

of the applied N-body method or configuration. The disadvantage that the conditions of the basic definition are idealized and rarely exactly fulfilled, seems to be less severe for a comparison of the softening schemes. Finally, a comparison with N-body calculations allows to check the applicability of the results with respect to both, realisitic particle configurations and collective relaxation effects.

In the next section the numerical procedure to get the relaxation times will be briefly explained and applied to the Keplerian potential as a test. In Sect. 3 the scheme will be applied to the Plummer and spline softening and compared with the Keplerian case. Additionally, a simple model for the influence of softening on the relaxation rates will be given. In Sect. 4 the results will be discussed and compared with N-body simulations.

2. Numerical method

2.1. The two-body relaxation time

Usually the two-body relaxation is quantified by a relaxation time (e.g. Spitzer 1987 Eq. (2-61))

$$\tau \equiv \frac{\sigma^2}{3\langle(\Delta v_\parallel)^2\rangle_{v=\sigma}} \,. \tag{4}$$

After this time τ the squared mean change of the velocity $v_\parallel$ parallel to the velocity of a test particle – moving with a velocity σ – is equal to $\sigma^2/3$, the mean squared velocity in any direction for an isotropic velocity distribution. Though there are also other possible definitions for a relaxation time, e.g. connected to the change rate of the energy itself (Chandrasekhar's T_E), I will restrict for the following analysis to the definition given in Eq. (4). In case of the Keplerian potential Chandrasekhar (1942) showed that the different definitions result in expressions varying not more than a factor of 2 for the relevant cases. For a homogeneous and isotropic stellar system Spitzer & Hart (1971) calculated the widely used expression for the relaxation time $\tau_{\rm rlx,h}$ at the half-mass radius r_h

$$\tau_{\rm rlx,h} = \frac{\sigma^3}{1.22 n_{\rm f} \Gamma} \tag{5}$$

where

$$\Gamma \equiv 4\pi G^2 {m_{\rm f}}^2 \ln\frac{p_{\rm max}}{p_0} \,. \tag{6}$$

$n_{\rm f}$ and $m_{\rm f}$ are the number density and mass of the field stars, respectively. The argument of the Coulomb logarithm is given by the ratio of a maximum impact paramater $p_{\rm max}$ and the 90° deflection impact parameter p_0 (Spitzer 1987, Eqs. (2-13) and (2-61)).

For a virialized system of equal mass particles Eq. (5) can be simplified to

$$\tau_{\rm rlx,h} = \frac{N}{26\log(0.4N)}\tau_{\rm d} \approx 0.04\frac{N}{\log(0.4N)}\tau_{\rm d} \,, \tag{7}$$

which relates the dynamical timescale $\tau_{\rm d} \equiv r_h/\sigma$ to the relaxation time by a factor only depending on the number N of particles in the system. A similar expression, with a different numerical factor, has already been derived by Chandrasekhar. Though Eq. (7) is not an exact result with respect to the definition (4) - as discussed later in Sect. 2.4 -, it allows for a fairly good and simple estimate of the importance of two-body relaxation on a given timescale.

2.2. Determination of change rates

According to Eq. (4) the determination of the relaxation time is basically the numerical evaluation of $\langle(\Delta v_\parallel)^2\rangle_{v=\sigma}$, i.e. the squared mean change rate of the velocity $v_\parallel$ parallel to the velocity of a test particle moving with a velocity σ. This quantity is calculated in three steps (for details see Appendix):

1. **Determination of the deflection angle χ of a two-body encounter in the potential**. For a given impact parameter p and a given relative velocity $v_{\rm rel}$ between the two interacting particles, the rate of change of the velocity $v_\perp$ perpendicular to $v_{\rm rel}$ is calculated by solving the equation of motion in the corresponding two-body problem.
2. **Averaging over the impact parameter range**. This procedure gives the average rate of change
$$\langle(\Delta v)^2\rangle_p = c(v_{\rm rel}, m_{\rm f}, m)\cdot n_{\rm f}\cdot D_\perp(p_{\rm max}, v_{\rm rel}) \tag{8}$$
of the velocity $v_\perp$ for a fixed relative velocity $v_{\rm rel}$ between the test particle of mass m and an arbitrary field particle. The constant c depends only on the initial relative velocity $v_{\rm rel}$ and the masses of the two particles (cf. Eq. (B5)). $D_\perp(p_{\rm max}, v_{\rm rel})$ is related to the impact parameter average of the deflection angle (cf. Eq. (B4)). The rate of change also includes the number density distribution of the field stars and thus the result depends on the exact location inside the N-body system. To avoid this additional free parameter, it is usual to assume a constant particle density which appears just as a factor in Eq. (8). However, this assumption leads to a divergence in the averaging process. For that reason, a maximum impact parameter $p_{\rm max}$ is introduced which is either related to the typical size of the whole system (e.g. Spitzer & Hart 1971, Farouki & Salpeter 1982, 1994) or to the mean interparticle spacing (e.g. Chandrasekhar 1942, Kandrup 1980, Smith 1992). Though there is still some debate about the proper choice of $p_{\rm max}$, the first choice seems to be more appropriate to explain the results of the N-body simulations shown later in this paper.
Also, a lower integration limit is frequently introduced, since in an approximation for the Keplerian potential a logarithmic divergence is found for small impact parameters. The corresponding limit is typically connected to the impact parameter $p_0 \equiv G(m + m_{\rm f})/{v_{\rm rel}}^2$ for a 90° deflection (e.g. Spitzer 1987). However, an exact integration gives no divergence at small impact parameters. Therefore, the result of the impact parameter averaging only depends on the two parameters $v_{\rm rel}$ and $p_{\rm max}$.
3. **Averaging over the velocity distribution of the field stars**. In the last step the component parallel to the incident velocity of the test particle has to be calculated and averaged over

the velocity distribution. Generally, the result depends on the distribution function. Here I will assume a Maxwell-Boltzmann velocity distribution, because it permits a direct comparison with previous work as well as it reduces the number of numerical integrations by one.

Since already the first step has to be done numerically for an arbitrary softened potential, all the other steps must also be performed numerically. In detail, the orbit integration is performed with a Runge-Kutta integrator of fourth order. The deflection angles are calculated on a logarithmically spaced grid in the (p,$v_{\rm rel}$)-space on 500x800 grid cells. The impact parameter ranges from $0.01p_0$ to $10^3\epsilon$. The logarithmic spacing assures an accurate resolution in each interval of $\log p/p_0$ which contributes almost equally to the cumulative deflection. Additionally, 100 logarithmically distributed points on the p-axis were chosen in the range $[0.1\epsilon, 10\epsilon]$ in order to get also a good resolution of the deflection curve close to the softening length ϵ (cf. Fig. 2).

In the next step the averaging over the impact parameter is done with the Romberg integration method. The resulting function $D_\perp(p_{\rm max}, v_{\rm rel})$ is tabulated by spline interpolation. In the final step the convolution of $D_\perp(p_{\rm max}, v_{\rm rel})$ and the velocity distribution is done again by Romberg integration.

2.3. Units

For the following calculations the gravitational constant G and the total mass $m + m_{\rm f}$ of the two interacting particles are normalized to unity. The Plummer softening ϵ is also set to unity. This choice allows to measure all length scales in Plummer softening lengths and all velocities in units of the escape velocity $v_{\rm esc} = \sqrt{2G(m+m_{\rm f})/\epsilon}$ of the 'reduced' particle.

2.4. Check with the Keplerian case

The accuracy of the numerical scheme is checked by the exact analytical solutions for the Keplerian potential. The relative error of the deflection angle was always better than 10^{-4}. Except for almost parabolic encounters, i.e. a deflection near 180°, the accuracy was even some orders of magnitude better. If $\chi \approx 180°$ the estimate of the real deflection angle by the tangent to the orbit becomes worse and might be improved by integrating to larger particle separations. However, due to the 8 Byte realization of FORTRAN double precision numbers the results cannot be improved reliably by more than two orders of magnitude at best. On the other hand, the 180° deflections are only important for small impact parameters which do not contribute significantly because of the impact parameter averaging.

The integration over the impact parameter was checked for the numerical solutions of the deflection angle determined in the first step. Therefore, I calculated the orbit averaged change rate $\langle(\Delta v)^2\rangle_p$ of the squared total velocity and compared it with the analytical result (Eq. (2-8) in Spitzer, 1987). For all maximum impact parameters $p_{\rm max}$ ranging from p_0 to $10^6 p_0$ the relative deviation was less than 10^{-6}.

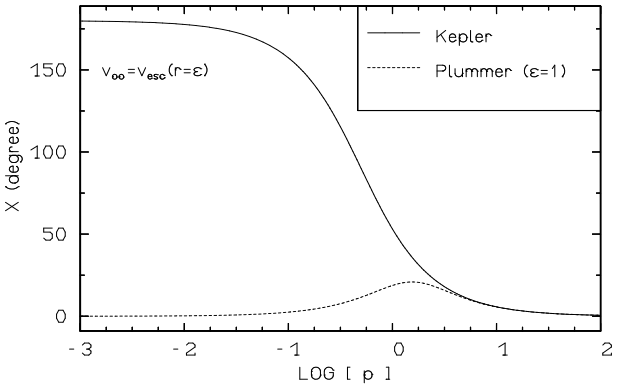

Fig. 2. Dependence of the deflection angle χ of the relative velocity $\boldsymbol{v}_{\rm rel}$ on the impact parameter p for a Plummer softened and a Keplerian potential. The modulus of $\boldsymbol{v}_{\rm rel}$ is set to the escape velocity $v_{\rm esc} = \sqrt{2G(m+m_{\rm f})/\epsilon}$ at the distance $r = \epsilon = 1$. The gravitational constant and the total mass of the two interacting particles are normalized to unity, whereas the length is measured by a unity Plummer softening length.

The accuracy of the last step was checked by the convolution of $\langle(\Delta v)^2\rangle_p$ with a Maxwell-Boltzmann velocity distribution, i.e.

$$\langle(\Delta v)^2\rangle_{p,v} = \int_0^\infty \langle(\Delta v)^2\rangle_p \cdot F_{\rm MB}(v) d^3v$$

$$= 8\sqrt{6\pi} \cdot \frac{G^2 n_{\rm f} {m_{\rm f}}^2}{\sigma_{\rm 3d,rel}} \cdot [-{\rm ci}(\beta)\cos(\beta) - {\rm si}(\beta)\sin(\beta)] \qquad (9)$$

with the distribution function

$$F_{\rm MB}(v_{\rm rel}) \equiv \sqrt{\left(\frac{3}{2\pi{\sigma_{\rm 3d,rel}}^2}\right)^3} \cdot \exp\left(-\frac{3{v_{\rm rel}}^2}{2{\sigma_{\rm 3d,rel}}^2}\right) \qquad (10)$$

for the relative velocity $v_{\rm rel}$ and

$$\beta \equiv \frac{3G(m+m_{\rm f})}{2p_{\rm max}{\sigma_{\rm 3d,rel}}^2} \cdot \qquad (11)$$

si and ci are the sine and cosine integrals. In the physically interesting regime (i.e. $p_{\rm max} \gg p_0$ or $\beta \ll 1$) the term in brackets in Eq. (9) can be expanded into $-\gamma - \ln(3/2) + \ln(p_{\rm max}/p_0)$ with Euler's constant $\gamma \approx 0.57721$. For the rates of change computed in this paper the agreement between the numerical results and the approximation (5) and (6) becomes better, if the Coulomb logarithm $\ln\Lambda \equiv \ln(p_{\rm max}/p_0)$ is corrected by -0.98 (see also Hénon (1975)).

With respect to the exact result Eq. (9) the relative error of the numerical solutions is always less than 10^{-4}. Though there are several different numerical steps, the result of each step and the total procedure is accurate enough to calculate reliable change rates numerically. Moreover, the Keplerian case is a 'worst case' model, because deflections are stronger than in a softened potential. For this reason, errors in the orbit integration – though they are not affecting the results in the Keplerian case

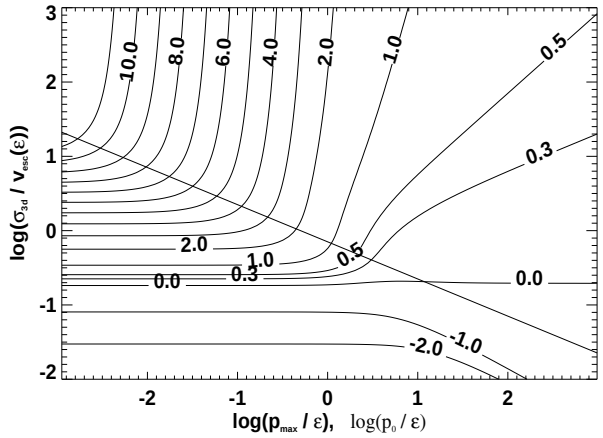

Fig. 3. The contour lines of $\log(\tau_{\rm soft}/\tau_{\rm Kepler})$ show the increase of the relaxation time in a Plummer softened potential compared to the corresponding value in a Keplerian potential as a function of the maximum impact parameter $p_{\rm max}$ (normalized to the softening length ϵ) and the velocity dispersion σ of the field stars. The velocity is normalized to the escape velocity of two interacting particles. The straight line shows the impact parameter p_0 for a 90° deflection as a function of the initial relative velocity $v_{\rm rel}$, assuming $v_{\rm rel} = \sigma$.

strongly – should become even smaller. However, in a softened potential the additional condition, that the orbit integration is not stopped before the separation r between the interacting particles is large compared to the softening length ϵ, must be fulfilled, whereas in the Keplerian case, r only has to be large compared to the minimum distance $r_{\rm min}$ between the particles.

3. Results

The main effect of gravitational softening is to decrease the force for small distances. This changes the behaviour of the deflection angles for small impact parameters p qualitatively: Whereas the divergence of the Keplerian potential results in a 180° deflection for decreasing p, the softening reduces the attracting force leading to a maximum of the deflection for impact parameters close to the softening length (Fig. 2). However, for large impact parameters the softened potential does not differ from the Keplerian.

The different softening procedures are compared by the increase of the relaxation times relative to the Keplerian potential, because this ratio only depends on the maximum impact parameter $p_{\rm max}$, the velocity dispersion σ of the field stars and the softening length ϵ. Moreover, the latter dependence can be absorbed by a proper choice of units, and so only the two parameters $p_{\rm max}$ and σ remain.

3.1. Plummer softening

Fig. 3 shows the logarithmic ratio $\log(\tau_{\rm Pl}/\tau_{\rm Kepler})$ of the relaxation time in a Plummer softened potential and the corresponding Keplerian value for a large range of maximum impact parameters $p_{\rm max}$ and velocity dispersions σ of the field stars. The straight line for the 90° deflection impact parameter p_0 splits the $p_{\rm max}$ -σ-plane into two parts: Below that line the maximum impact parameter is smaller than p_0, i.e. the typical size of the system is of the order of p_0. In a system of equal mass particles this is only possible for a very small number N of particles, since they are expected to be almost bound pairwise. Obviously, this is an unphysical regime even for a moderate $N \approx 20$[1].

The largest increase of the relaxation time by softening is in the region for small $p_{\rm max}$ and large velocities. However, also this case is physically irrelevant, since the potential would be modified on the scale of the whole system.

Physically interesting is only the region for $p_{\rm max} > \epsilon$ and $\sigma > v_{\rm esc}$, i.e. the upper right of Fig. 3. One can specify this region more closely, if one assumes (as done by many authors) that the softening length is scaled by the mean interparticle distance or $\epsilon \approx R \cdot N^{-1/3}$. In case of Plummer softening Merritt (1996) showed that for a dynamically hot system this choice is qualitatively the best with respect to resolution and a collisionless behaviour of the N-body system. However, the exact dependence might deviate from the simple $N^{-1/3}$ scaling. If one additionally assumes virial equilibrium, the velocity dispersion of a system with total mass M can be estimated by $\sigma^2 \approx GM/R$. Together with the escape velocity $v_{\rm esc} = \sqrt{2G(M/N)/\epsilon}$ one gets

$$\begin{aligned} \frac{\sigma}{v_{\rm esc}} &= \frac{1}{\sqrt{2}} \cdot N^{1/3} \\ \frac{p_{\rm max}}{\epsilon} &= N^{1/3} \end{aligned} \qquad (12)$$

Thus, the physically interesting region scales only weakly with the number of particles. Even if we omit the assumption of the relation between the softening length and the interparticle distance, ϵ should not become larger than $R/10$ and $\log(p_{\rm max}/\epsilon)$ would not drop below +1. An enlargement of this region is shown in Fig. 4, where the contour lines give the linear instead of the logarithmic ratio: The softening increases the relaxation time less than one order of magnitude. Larger increases are only found in the non-physical regimes which are either not appropriate for a N-body system or modify the gravitational force too strongly. An increase of the number of particles does not change this picture qualitatively as the scaling relations (12) demonstrate. The same holds for an increase of the softening length, if it remains smaller than the size of the system.

3.2. Spline softening

In order to allow for a comparison between the spline based softening and the Plummer softening, the softening length $\epsilon_{\rm sp}$

[1] For small velocity dispersions the relaxation time becomes even shorter by softening! However, this is an artificial effect caused by the definition of the relaxation time in Eq. (4) and the terms used for calculating $\langle(\Delta v_\parallel)^2\rangle_{v=\sigma}$ according to Spitzer's definition (1987) (cf. Eq. (B1)). In that expression the 'usually' dominant term is the change $v_\perp$ of the velocity perpendicular to the initial relative velocity. However, for small relative velocities, the deflections are close to 180° and the assumption of a negligibly small parallel component of the velocity change is no longer valid.

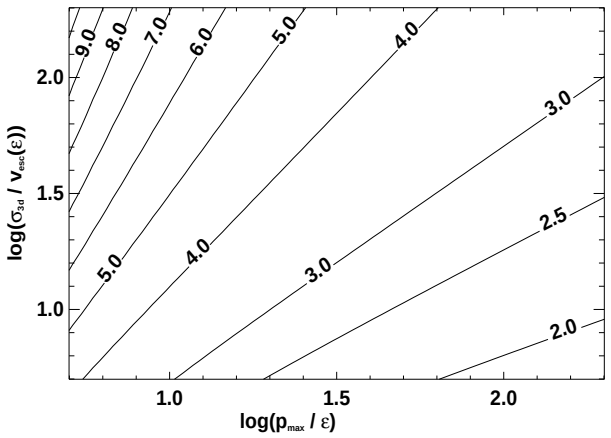

Fig. 4. This diagram is a blow-up of Fig. 3 showing the physically interesting region. However, the contour lines here give the ratio $\tau_{\rm soft}/\tau_{\rm Kepler}$ directly (see also caption of Fig. 3).

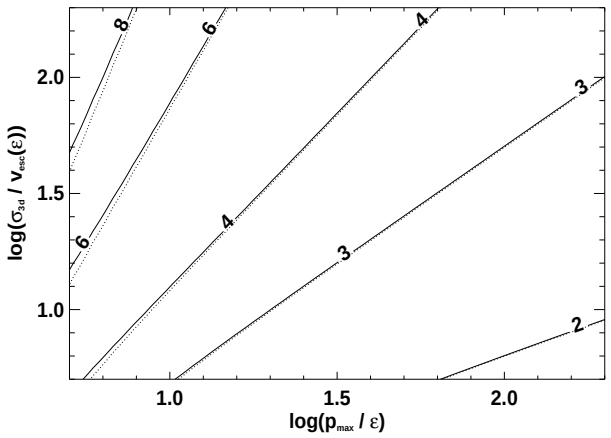

Fig. 6. The contour lines show the ratio $\tau_{\rm soft}/\tau_{\rm Kepler}$ of the relaxation times of a softened potential and the Keplerian potential, for both a Plummer softened (solid) and a spline softened potential with $\epsilon_{\rm sp} = 2\epsilon$ (dotted) (see also caption of Fig. 3).

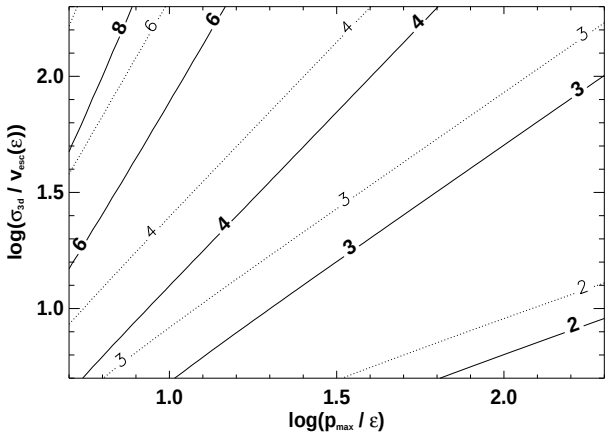

Fig. 5. The contour lines show the ratio $\tau_{\rm soft}/\tau_{\rm Kepler}$ of the relaxation times of a softened potential and the Keplerian potential, for both a Plummer softened (solid) and a spline softened potential with $\epsilon_{\rm sp} = 1.4\epsilon$ (dotted) (see also caption of Fig. 3).

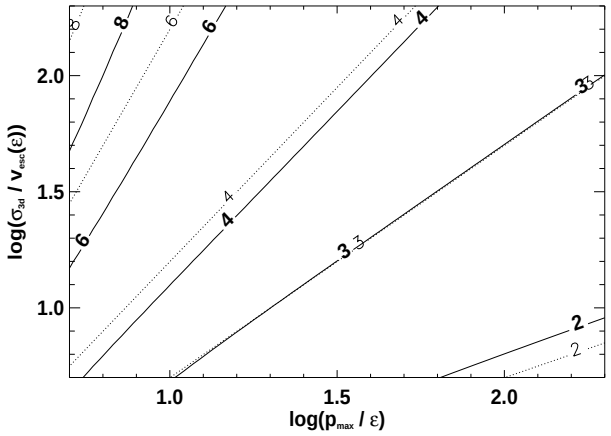

Fig. 7. The contour lines show the ratio $\tau_{\rm soft}/\tau_{\rm Kepler}$ of the relaxation times for a Plummer softened potential (solid) and the corresponding values of the simple model (dotted) (see also caption of Fig. 3).

was set to $7/5 \cdot \epsilon$. This choice gives the same central potential depth for both softening methods. For a value $\epsilon_{\rm sp} = \epsilon$, the potential wall for the spline softening becomes deeper leading to a stronger scattering and a shorter relaxation time anyway.

The results for the spline based softening are qualitatively the same as for the Plummer softening. In detail, however, the spline softening is slightly 'grainier' as the comparison of both procedures for fixed central potential demonstrates (Fig. 5). The relaxation times become almost identical, if $\epsilon_{\rm sp}$ is set to 2ϵ (Fig. 6). In a first order approximation this ratio can be estimated within 10% by the softening ratio at which the difference of the volume averaged forces, $\propto \int r(\phi_{\rm P}(r) - \phi_{\rm S}(r))\, dr$, vanishes. Therefore, keeping the relaxation times constant the nominal spatial resolution represented by the softening length is a factor 2 smaller for the spline based scheme.

4. Discussion

4.1. A simple model

To understand the behaviour of the relaxation time ratios of the previous section, let us assume the following simple model: For impact parameters p smaller than the softening length ϵ , there should be no deflection, whereas for $p > \epsilon$ the deflection should be identical to the Keplerian case. Then the change of the relative velocity can be expressed by

$$\langle(\Delta v)^2\rangle_{p_{\rm simple}} \approx C \cdot \ln\left(\frac{p_{\rm max}}{\epsilon}\right) , \tag{13}$$

whereas one gets for the Keplerian case (Spitzer, 1987)

$$\langle(\Delta v)^2\rangle_{p} \approx C \cdot \ln\left(\frac{p_{\rm max}}{p_0}\right) . \tag{14}$$

Table 1. N-body simulations. Tabulated are the model name (col. 1), the softening length ϵ (col. 2), the numerical timestep Δt (col. 3), the opening angle θ (col. 4), the application of quadrupole terms (col. 5) (both only for tree-code calculations), the form of the particle interaction (col. 6), the measured particle energy dispersion σ_E (col. 7), the measured ratio of the relaxation times normalized to the Keplerian case (col. 8) and the corresponding analytical value (col. 9).

model	ϵ	Δt	θ	quadrupole	potential	σ_E	$\left(\sigma_{E,\,\mathrm{Kep}}/\sigma_E\right)^2$	
							num.	analyt.
A1	0.0	0.001	–	–	Keplerian potential	0.282	1	–
A2	0.0	0.0001	–	–	Keplerian potential	0.275	1.05	–
B1	0.042	1/40	–	–	Plummer softening	0.128	4.89	4.66
B2	0.042	1/80	–	–	Plummer softening	0.132	4.59	4.66
C1	0.021	1/40	–	–	Plummer softening	0.171	2.73	3.19
C2	0.021	1/80	–	–	Plummer softening	0.165	2.92	3.19
C3	0.021	0.001	–	–	Plummer softening	0.167	2.87	3.19
D1	0.042	1/40	0.7	yes	spline softening	0.168	2.82	3.21
D2	0.042	1/80	0.7	yes	spline softening	0.162	3.03	3.21
D3	0.042	1/40	0.7	no	spline softening	0.171	2.71	3.21
D4	0.042	1/40	0.5	yes	spline softening	0.170	2.77	3.21
D5	0.042	1/40	1.0	yes	spline softening	0.169	2.77	3.21
E1	0.021	1/40	0.7	yes	spline softening	0.206	1.87	2.42
E2	0.021	1/80	0.7	yes	spline softening	0.197	2.04	2.42
F1	0.0588	1/40	0.7	yes	spline softening	0.148	3.62	3.81

The constant C is equal for both change rates. Thus, the increase R of the relaxation time according to this simple model is given by

$$R = \frac{\ln \frac{p_{\max}}{p_0}}{\ln \frac{p_{\max}}{\epsilon}} \tag{15}$$

and the corresponding contour lines are

$$\log \frac{\sigma}{v_{\mathrm{esc}}} = -\frac{1}{2}\log 2 + \frac{R-1}{2}\log \frac{p_{\max}}{\epsilon}\,. \tag{16}$$

They give a good qualitative agreement with the exact integrations and their slopes $(R-1)/2$ are even in quantitative agreement (Fig. 7). The systematic deviation increasing with R is caused by the replacement of the exact integration over the Maxwell-Boltzmann velocity distribution with using the velocity dispersion. Performing the integration over velocity space gives a constant deviation of the contour lines with respect to the softened potentials, i.e. the systematic trend is removed.

The simple model is in qualitative agreement with the suggestion by White (1978) to replace the Coulomb logarithm by $\ln(p_{\max}/(1.65\epsilon))$ in the case of Plummer softening. This is equivalent to assume a lower cut-off in the simple model at 1.65ϵ instead of ϵ. However, such an 'effective softening length' should be applied carefully, since the calculations show that there is no unique value for the whole $p_{\max} - \sigma$-plane.

In order to increase the relaxation time there are generally two ways: First, one may increase the softening length ϵ which means to move on a line of slope -1/2 in a diagram like Fig. 3. However, even a change of ϵ by one order of magnitude increases the relaxation time only by a factor 2-3. An alternative possibility is to use more particles which means to move on a line of slope +1, if the softening length varies according to the mean interparticle distance (cf. Eq. (12)). In that case Eq. (16) shows that the ratio R of relaxation times will only be increased if $R < 3$, otherwise it will even be decreased. A change of N by a factor 10 leaves R almost constant, whereas the absolute value of the relaxation time varies strongly. Finally, if N is increased by an order of magnitude keeping ϵ constant, the ratio of relaxation times will always be increased, but only by a factor 1.5-2.

4.2. Mass dependence

The mass dependence of the relaxation time is given by Eqs. (5) and (6). E.g. an enhancement of the mass of the field particles by a factor 10 with respect to the test particles, decreases the relaxation time by one order of magnitude, if the mass density of the field stars is kept constant. However, the ratio between the relaxation times for the Keplerian and a softened potential is unchanged, since the mass ratio does not affect the Coulomb logarithm and thus the ratio of the velocity change rates. For the Keplerian potential this is obvious, because the impact parameter p_0 for a 90° deflection does not depend on the mass ratio, but on the total mass of the two interacting particles. Hence, the Coulomb logarithm $\ln(p_{\max}/p_0)$ is unchanged, if we normalize to our units. This means that the Figs. 3-7 are the same even if the masses of the test particle and the field particles differ.

However, this does not mean that the relaxation times measured in a N-body simulation should not depend on the mass ratio, since the softening might also affect the overall structure of the N-body system resulting in different density profiles and, therefore, in different 'true' relaxation times. E.g. in a two-mass system the scale length of the lighter component might exceed the softening length after energy equipartition, whereas the heavier component could be more strongly affected due to its smaller scaleheight. This is not expected to result in general

in the same relaxation time as in an equal mass system with a different scaleheight and thus a different ratio of $p_{\max}/\epsilon$.

4.3. Comparison with N-body simulations

In a series of N-body calculations the semi-analytical results are compared with numerical simulations applying the Plummer softening (model series B and C), the spline based softening (D, E and F) and the pure Keplerian (A) potential (Tab. 1). In all these models I distributed $N = 4096$ particles according to a Plummer mass distribution in virial equilibrium and followed their evolution over 20 crossing timescales $\tau_{\rm cr} \equiv GM^{2.5}/\sqrt{2|E|}^3$ (E is the total energy of the system). The scale radius r_0 of the Plummer model was set to $r_0 = \sqrt[3]{27\pi^3/32768} \approx 0.2945$ resulting in a unity crossing time. The initial particle distribution was generated according to the method described in Aarseth et al. (1974). The measurements were started after the system relaxed for 10 crossing times in order to avoid additional relaxation due to global instabilities arising from a 'non-quiet' start. Using Eq. (7) one expects a relaxation time of $\tau_{\rm rlx,h} \approx 51\tau_{\rm d}$ in the Keplerian case. Therefore, relaxation effects should be clearly detectable after 20 $\tau_{\rm d}$, but they do not have enough time to change the structure of the N-body system strongly and a comparison between softened and non-softenend calculations is possible. The relaxation rate was quantified by the dispersion σ_E of the individual particle energies (Hernquist & Barnes 1990)

$$\sigma_E \equiv \left[\frac{1}{N-1} \cdot \sum_{k=1}^{N} \left(\frac{\Delta E_k}{E_{k,\rm ini}} - \overline{\Delta E} \right)^2 \right]^{1/2} \tag{17}$$

with the mean energy change

$$\overline{\Delta E} \equiv \frac{1}{N} \cdot \sum_{k=1}^{N} \frac{\Delta E_k}{E_{k,\rm ini}} \,. \tag{18}$$

$E_{k,\rm ini}$ is the initial energy of particle k and ΔE_k its final energy difference with respect to the initial value.

The simulations with the Plummer softening and the Keplerian model were performed with a GRAPE3af special purpose computer (Sugimoto et al. 1990). The simulations for the spline softening are done with a tree-code on a general purpose computer (Hernquist 1987). A constant timestep Δt was chosen to 1/40 $\tau_{\rm cr}$ or less. In all models with softening the energy conservation was better than 0.5%, in most cases much better. In the calculations with a pure Keplerian potential (models A1 and A2) the energy conservation was 6% and 2%. Though the energy conservation is worse than in the simulations including softening, the relaxation rates measured by σ_E differ only by 5%. Therefore, the model A1 will be used as the reference Keplerian model and the typical error due to the time integration scheme is estimated by model A2 to be of the order of 5%. In all the models the Lagrange radii between 0.1% and 95% of the total mass remain constant within statistical errors.

In order to estimate the energy dispersion σ_E, I fitted the temporal evolution of $\sigma_E(t)$ by a diffusion ansatz ($\sigma_E(t) \propto \sqrt{t}$) for the data between 10 and 20 $\tau_{\rm cr}$. The coefficient of regression exceeds always 99%, indicating that the data are well represented by the diffusion model, as already found by Hernquist & Barnes (1990). Thus $\left(\frac{\sigma_{E,\rm Kep}}{\sigma_E}\right)^2$ allows an estimate for the increase R of the relaxation time by softening. These values are given in Tab. 1 and compared with the analytical model assuming a maximum impact parameter $p_{\max} = r_0$. In all the models R is less than 5 in agreement with the prediction that the increase of the relaxation time is moderate, if the softening length is of the order of the mean interparticle spacing.

Though the numerical results depend on the chosen timestep, they do not differ by more than 8% (A1-A2, B1-B2, C1-C3, D1-D2, E1-E2). The same holds for other 'technical' parameters like the opening angle θ (D1, D4, D5) or the use of the quadrupole moments (D1, D3) in the tree-code simulations (Hernquist 1987). For all the simulations there is a fair agreement with the analytical results. The differences of up to only 20% are not too bad, because many of the assumptions made in the analytical model are not fulfilled by the initial N-body configuration: non-constant density profile, non-Gaussian velocity distribution. Additionally, there is some noise in the N-body data and thus in the energy deviations. And, last but not least, calculating the energy deviation does not match exactly the definition for the relaxation time based on the change rate of the velocity component parallel to the incident velocity of a test particle. However, none of these points is expected to change the predictions qualitatively.

If one compares the Plummer softening with a spline based scheme, the relaxation time in the latter is smaller (B1-D1, C1-E1). In agreement with the analytical models, this is even true if the softening length $\epsilon_{\rm sp}$ in the spline based softening exceeds the Plummer softening length by a factor 7/5, i.e. both have identical central potential depths (B1-F1). Hence the spline based softening is slightly 'grainier' than the Plummer one. If $\epsilon_{\rm sp} = 2\epsilon$ the semi-analytical models predict that the relaxation times should be almost identical. Thus, the pairs (C1-D1) and (C2-D2) should have identical relaxation rates which is found within less than 4% deviation for both sets of models.

The reasonable agreement between semi-analytical models and the N-body calculations shows that the relaxation rates in these simulations can be mainly explained by local two-body encounters. Thus, collective relaxation seems not to contribute significantly to the relaxation rates measured by the numerical models. Additionally, an initial transitory phase – if existing – seems not to be important here, as the agreement ($< 10\%$) of the relaxation rates measured without waiting for 10 crossing times, demonstrates.

5. Conclusions

Semi-analytical calculations for the two-body relaxation in softened potentials are presented. They show that the increase of the relaxation time due to softening is generally less than one order of magnitude, typically between 2 and 5, if the softening length is approximately equal to the mean interparticle distance. They

might be slightly larger, if the softening length is a large fraction of the system's size, which would give a bad spatial resolution, if it is appropriate at all. An increase of the particle number does not increase the ratio of relaxation times for softened and Keplerian potentials significantly, though the absolute values vary strongly.

A comparison of the Plummer softening with a spline based softening shows that the latter one is grainier as well for the same softening length as for a softening length increased by a factor 1.4 in order to have the same central potential depth in both schemes. However, quantitatively these differences are small. If the softening length for the spline based softening is chosen to be twice the value for the Plummer softening, the relaxation times become almost identical. N-body simulations using different softening schemes and lengths are in fair agreement with these results.

The main effect of softening can be well described by a simple model assuming that softening suppresses all deflections, if the impact parameter is smaller than ϵ, and otherwise gives the Keplerian deflection. This allows for a quick estimate of the influence of softening with respect to cumulative two-body relaxation. Moreover, the good agreement of the simple model with the N-body calculations implies that the upper limit of the impact parameter $p_{\max}$ should be connected to the size of the system instead of the mean interparticle distance. Otherwise, the denominator in Eq. (15) would become very small and the increase of relaxation time should be much larger, which is in in contradiction to the N-body results. Therefore, a choice of $p_{\max}$ of the order of the system's size instead of the mean interparticle distance seems to be more appropriate corroborating the results of Farouki & Salpeter (1982, 1994).

Acknowledgements. I want to thank Douglas Heggie, Rainer Spurzem, David Merritt and Ortwin Gerhard for comments and discussions about relaxation. Also the detailed remarks of the referee, Alessandro Romeo, are gratefully acknowledged. For a careful reading of the manuscript I'm gratefully indebted to J. Köppen and T. Freyer. The simulations were partly performed with the GRAPE3af special purpose computer in Kiel (DFG Sp345/5), and partly by using the TREEcode kindly made available by Lars Hernquist. The author gratefully acknowledges the support by the TRACS programme and the hospitality of the Edinburgh Parallel Computing Center and the Dept. of Mathematics and Statistics of the University of Edinburgh.

Appendix A: orbit equation

For a central force problem the orbit equation is given by (e.g. Goldstein, 1980)

$$\frac{d^2u}{d\theta^2} + u = -\frac{m_{\rm red}}{l^2u^2} \cdot F(1/u) \tag{A1}$$

$u \equiv 1/r$ is the inverse of the distance r between both particles and $l \equiv m_{\rm red}\, p\, v_\infty$ the angular momentum of the particle with the reduced mass $m_{\rm red} = (m_{\rm f} m)/(m_{\rm f} + m)$. The interaction is characterized by the impact parameter p and the relative velocity v_∞ at infinity (Fig. 8). $F(1/u)$ is the force exerted by the potential on the 'reduced' particle, i.e. $-m_{\rm red}\partial\phi(1/u)/\partial r$. Because of the symmetry to changing the sign of θ the integration was started at the minimum separation $r_{\min}$. $r_{\min}$ is determined by solving the energy equation at $r_{\min}$ numerically

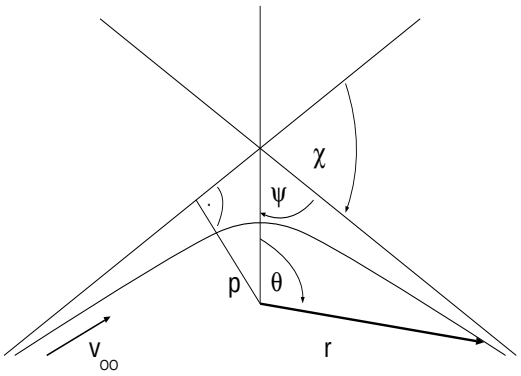

Fig. 8. Scheme of the two-body interaction

$$v_\infty{}^2 \cdot \left(1 - \frac{p^2}{r_{\min}{}^2}\right) - \phi(r_{\min}) = 0\,. \tag{A2}$$

The integration is stopped when the relative deviation of the deflection angle χ measured by the tangent to the orbit deviates less than 10^{-4} from the corresponding Keplerian value, but not before the distance r exceeds both $1000 r_{\min}$ and 1000ϵ. The latter ensures that the orbit determination is not stopped before it is almost a Keplerian one and, thus, the accuracy can be estimated by a comparison with the corresponding Keplerian orbit.

The change of the velocity of the test particle can now be expressed by the deflection angle, e.g. the component perpendicular to the initial velocity is given by

$$\Delta v_\perp = \frac{m_{\rm f}}{m + m_{\rm f}} v_\infty \sin\chi\,. \tag{A3}$$

Appendix B: impact parameter average

Spitzer (1987) showed that the dominant term contributing to the diffusion coefficient responsible for the relaxation is related to the velocity and impact parameter averaged change rate of the squared perpendicular velocity change $\Delta v_\perp$:

$$\langle \Delta v_i \Delta v_j \rangle = \int \frac{1}{2} \Xi_{ij} \langle (\Delta v_\perp)^2 \rangle_p \frac{f(\boldsymbol{v}_{\rm f})}{n_{\rm f}} d^3\boldsymbol{v}_{\rm f} \tag{B1}$$

f is the distribution function in $\boldsymbol{r}$ and $\boldsymbol{v}$ space, and therefore, $f(\boldsymbol{v}_{\rm f})/n_{\rm f}$ gives the velocity distribution function. The velocities v_i and v_j are related to a coordinate system $\boldsymbol{\epsilon}_i$ of the initial velocity $\boldsymbol{v}_{\rm ini}$ of the test particle (which is also used in the definition of the relaxation time). However, the velocity change calculated by Eq. (A1) is related to the different coordinate system $\tilde{\boldsymbol{\epsilon}}_i$ of the initial relative velocity $\boldsymbol{v}_{\rm rel}$ of the two interacting particles. Thus, the velocity change is transformed to the reference frame of the test particle. Assuming that the first coordinate direction of the $\tilde{\boldsymbol{\epsilon}}$-system is aligned with $\boldsymbol{v}_{\rm rel}$ the quantity

$\Xi_{ij} \equiv (\boldsymbol{\epsilon}_i \cdot \tilde{\boldsymbol{\epsilon}}_2)(\boldsymbol{\epsilon}_j \cdot \tilde{\boldsymbol{\epsilon}}_2) + (\boldsymbol{\epsilon}_i \cdot \tilde{\boldsymbol{\epsilon}}_3)(\boldsymbol{\epsilon}_j \cdot \tilde{\boldsymbol{\epsilon}}_3)$ transforms the perpendicular component of the change of $\boldsymbol{v}_{\rm rel}$ to the test particle's reference frame. Assuming additionally that the direction of the first coordinate of the $\boldsymbol{\epsilon}$-system is parallel to $\boldsymbol{v}_{\rm ini}$, one gets

$$\begin{aligned}\langle(\Delta v_\parallel)^2\rangle &= \langle \Delta v_1 \Delta v_1 \rangle \\ &= \pi \frac{{m_{\rm f}}^2}{(m+m_{\rm f})^2} \cdot \qquad \text{(B2)} \\ &\quad \int (1-\cos^2\vartheta) \cdot D_\perp(p_{\rm max}, v_{\rm rel}) \cdot {v_{\rm rel}}^3 f(\boldsymbol{v}_{\rm f}) d^3\boldsymbol{v}_{\rm f} \\ &= 2\pi^2 \frac{{m_{\rm f}}^2}{(m+m_{\rm f})^2} \cdot \int_0^\infty D_\perp(p_{\rm max}, v_{\rm rel}) {v_{\rm rel}}^5 \cdot \qquad \text{(B3)} \\ &\quad \int_{-1}^{+1} (1-z^2) f(|\boldsymbol{v}_{\rm ini} + \boldsymbol{v}_{\rm rel}|) dz dv_{\rm rel} \,.\end{aligned}$$

ϑ is the angle between $\boldsymbol{v}_{\rm ini}$ and $\boldsymbol{v}_{\rm rel}$. In the latter equation it is assumed that the velocity distribution of the field stars depends only on the modulus of the velocity, i.e. the velocity distribution is isotropic. The quantity

$$D_\perp(p_{\rm max}, v_{\rm rel}) \equiv \int_0^{p_{\rm max}} \sin^2\chi(p, v_{\rm rel}) p dp \qquad \text{(B4)}$$

is related to the impact averaged $\Delta v_\perp$ by

$$\langle(\Delta v_\perp)^2\rangle_p = D_\perp(p_{\rm max}, v_{\rm rel}) \cdot \left(\frac{m_{\rm f}}{m+m_{\rm f}}\right)^2 \cdot {v_{\rm rel}}^3 \cdot 2\pi n_{\rm f} \,. \qquad \text{(B5)}$$

(Cf. also to Eqs. (2-18) and (2-20) in Spitzer (1987), but for a relative velocity distribution instead of a fixed relative velocity).

Appendix C: convolution with the velocity distribution

Partly, the convolution with the Maxwell-Boltzmann distribution, can be done explicitly:

$$\begin{aligned}\langle(\Delta v_\parallel)^2\rangle &= 2\pi^2 \left(\frac{m_{\rm f}}{m+m_{\rm f}}\right)^2 \cdot n_{\rm f} \sqrt{\left(\frac{3}{2\pi\sigma^2}\right)^3} \exp(-\frac{3{v_{\rm ini}}^2}{2\sigma^2}) \cdot \\ &\quad \int_0^\infty D_\perp(p_{\rm max}, v) v^5 \exp(-\frac{3v^2}{2\sigma^2}) \cdot G(\mu) dv \qquad \text{(C1)}\end{aligned}$$

with

$$G(\mu) \equiv \frac{2}{\mu^3}[(\mu+1)e^{-\mu} + (\mu-1)e^{\mu}] \qquad \text{(C2)}$$

and

$$\mu \equiv \frac{3 v v_{\rm ini}}{\sigma^2} \qquad \text{(C3)}$$

σ is the 3d velocity dispersion of the field stars. According to Spitzer's definition (4) of the relaxation time $\langle(\Delta v_\parallel)^2\rangle$ has to be evaluated for $v_{\rm ini} = \sigma$. Though the exact values for the relaxation time depend on many parameters like the mass of the particles or their densities, the ratio of the relaxation times in the Keplerian and in a softened potential depends only on the integral in Eq. (C1). Hence, the increase of the relaxation time can be characterized by the maximum impact parameter $p_{\rm max}$ and the velocity dispersion σ of the field stars. Another parameter, the softening length ϵ, can be normalized to unity by a proper choice of units.

The mass dependence in Eq. (C1) seems to contradict the standard relations (5) and (6) for the relaxation time. However, the denominator $(m+m_{\rm f})^2$ in (C1) cancels with the same expression in the numerator, if the integral in Eq. (B4) is written in a dimensionless form, e.g. by normalizing p to the 90° deflection impact parameter p_0. By this, the usual mass dependence is recovered.

References

Aarseth S.J., 1963, MNRAS, 126, 223
Aarseth S.J., Hénon M., Wielen R.: 1974, A&A, 37, 183
Chandrasekhar S., 1942, *Principles of Stellar Dynamics*, The Univ. of Chicago Press
Clutton-Brock M., 1973, Ap&SS, 23, 55
Farouki R.T., Salpeter E.E., 1982, ApJ, 253, 512
Farouki R.T., Salpeter E.E., 1994, ApJ, 427, 676
Goldstein H., 1980, *Classical Mechanics*, Addison Wesley Publ. Comp.
Hénon M., 1975, in *Dynamics of Stellar Systems*, IAU Symp. 69, Reidel, p. 133
Hernquist L., 1987, ApJS, 64, 715
Hernquist L., Barnes J., 1990, ApJ, 349, 562
Hernquist L., Katz N., 1989, ApJS, 70, 419
Hernquist L., Ostriker J.P., 1992, ApJ, 386, 375
Hohl F., 1973, ApJ, 184, 353
Junqueira S., Combes F., 1996, A&A, 312, 703
Kandrup H.E., 1980, Phys. Rep. 63, 1
Merritt D., 1996, AJ, 111, 2462
Mishurov Yu.N., 1984, SvA 28, 628
Pfenniger D., Friedli D., 1993, A&A, 270, 561
Quinn P.J., Hernquist L., Fullagar D.P., 1993, ApJ, 403, 74
Romeo A.B., 1994, A&A, 286, 799
Romeo A.B., 1997, A&A, 324, 523
Rybicki G.B., 1971, Ap&SS, 14, 15
Spitzer L., 1987, *Dynamical Evolution of Globular Clusters*, Princeton Univ. Press
Spitzer L., Hart M.H., 1971, ApJ, 164, 399
Sugimoto D., Chikada Y., Makino J., Ito T., Ebisuzaki T., Umemura M., 1990, Nat, 345, 33
Theuns T., 1996, MNRAS, 270, 827
van Albada T.S., 1986, in *The Use of Supercomputers in Stellar Dynamics*, eds. P. Hut & S. McMillan, Springer, p. 23
Weinberg M.D., 1993, ApJ, 410, 543
White R.L., 1988, ApJ, 330, 26
White S.D.M., 1978, MNRAS, 184, 185

This article was processed by the author using Springer-Verlag LaTeX A&A style file *L-AA* version 3.